Chemistry & Biology, Vol. 12, 1093–1101, October, 2005, ©2005 Elsevier Ltd All rights reserved. DOI 10.1016/j.chembiol.2005.08.007

A Tailoring Activity Is Responsible for Generating Polyene Amide Derivatives in *Streptomyces diastaticus* var. 108

Elena M. Seco,[1] Serge Fotso,[2] Hartmut Laatsch,[2] and Francisco Malpartida[1,*]
[1]Centro Nacional de Biotecnología
Campus de la Universidad Autónoma de Madrid
Cantoblanco
28049 Madrid
Spain
[2]Department of Organic and Biomolecular Chemistry
University of Göttingen
Tammannstrasse 2
37077 Göttingen
Germany

Summary

We recently characterized rimocidin B (3b) and CE-108B (4b) as two polyene amides with improved pharmacological properties, produced by genetically modified *Streptomyces diastaticus* var. 108. In this work, genetic and biochemical analysis of the producer strain show that the two amides are derived from the parental polyenes rimocidin (3a) and CE-108 (4a) by a post-PKS modification of the free side chain carboxylic acid. This modification is mediated by an amidotransferase activity operating after the biosynthesis of rimocidin (3a) and CE-108 (4a) are completed. Two polyenes, intermediates of the biosynthetic pathway of rimocidin (3a) and CE-108 (4a), were also isolated and shown to have some improved pharmacological properties compared with the final products.

Introduction

Polyenes are a large group of polyketides with antifungal activities, and they include antibiotics such as amphotericin B (**1**), pimaricin (**2a**), rimocidin (**3a**) (Figure 1), nystatin A1, and candicidin, all of which are biosynthesized by multifunctional proteins known as Type I modular polyketide synthases. The biological activity of these compounds, and thus their pharmacological properties, rely on the selectivity of their binding to membrane-associated substituted sterols such as ergosterol or episterol (found in the fungal cytoplasmic membrane or in some parasitic protozoa) [1–4]. As a result of these interactions, a multimolecular polyene/sterol complex is formed, leading to impairment of plasma membrane functions and, thus, cell death. Although the affinity of the polyene macrolides for cholesterol-containing membranes is low, it is not low enough to avoid the toxic side effects of some of these drugs. In spite of these limitations, amphotericin B (**1**) is still the preferred clinical drug for treating systemic fungal infections.

In order to gain insight into the structure/activity relationship, many semisynthetic derivatives of amphotericin B (**1**) were generated in the last decade [5–12]. Both the amino group of the sugar moiety and the side chain carboxyl group were targeted, and their influence on the biological properties of this compound is starting to be understood. Most of the semisynthetic compounds were generated by molecular modeling of amphotericin B (**1**), and this modeling was aimed at increasing the selective toxicity for ergosterol-containing membranes. Thus, amphotericin B (**1**), an efficient, old antifungal drug, became a standard for the successful generation of new analogs that had increased specificity for their targets but retained pharmacokinetic properties at least equivalent to those of the parent molecule. These findings make the macrolide polyenes an attractive model by which to attempt to increase the supply of lead compounds to fight serious fungal diseases.

Recently, we isolated *Streptomyces diastaticus* var. 108 as a producer of two polyene macrolides, rimocidin (**3a**) and CE-108 (**4a**) (Figure 1) [13]. A genetically modified derivative of this strain was shown to produce two new, to our knowledge, polyene macrolides: rimocidin B (**3b**) and CE-108B (**4b**) (Figure 1). In both compounds, the free carboxyl group is substituted by an amide, leading to compounds with lower toxicity, as indicated by their low hemolytic activity and higher antifungal properties [14]. Because of the importance of the novel compounds as putative new leads, the biosynthetic steps leading to this substitution were investigated in more detail. At least two possible mechanisms were suggested: (a) an amidotransferase acting as a tailoring activity after the complete macrolactone rings were generated; and (b) nondecarboxylating Claisen condensation of malonamide during the growth of the polyketide chain. It is noteworthy that the producer strain can also synthesize oxytetracycline [13]; thus, malonamyl-CoA must be available as the starter unit for biosynthesis of this aromatic polyketide [15].

Insights into the biosynthetic mechanism, described here, will be extremely useful in designing a strategy for genetic engineering of *S. diastaticus* var. 108 and perhaps other polyene producers in an attempt to obtain new pharmaceuticals.

Results

Elucidation of the Biosynthetic Mechanism for the Polyene Amides

To discriminate between the two possible mechanisms for polyene amide formation, a genetic approach was taken. Whatever the mechanism is, the role of the cytochrome P450 monooxygenase RimG, claimed to be responsible for oxidation of the side chain methyl group generated after condensation of methylmalonyl-CoA units by module 7 [14], must be crucial. If an amidotransferase activity is needed for amide formation, it must presumably operate after the side chain methyl group has been converted into the carboxyl group by the *rimG* product; on the other hand, if the amide group is incorporated by condensation of malonamyl-CoA during chain assembly, the *rimG* gene would not be

*Correspondence: fmalpart@cnb.uam.es

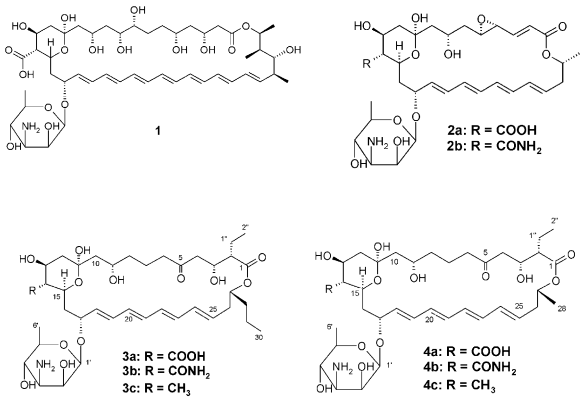

Figure 1. Chemical Structures of Polyenes that Are Cited within the Text

1, amphotericin B; **2a**, pimaricin; **2b**, AB-400; **3a**, rimocidin; **3b**, rimocidin B; **3c**, rimocidin C; **4a**, CE-108; **4b**, CE-108B; **4c**, CE-108C.

needed for amide group formation. The presence or absence of polyene amides in the fermentation broth of a *rimG* disruptant when a plasmid involved in the polyene amide biosynthesis is cloned into it should indicate the correct mechanism. We therefore attempted disruption of the *rimG* gene by insertional inactivation.

Because *rimG* lies within a long polycistronic transcript of 9 kbp, which also contains *rimE*, *rimF*, *rimG*, *rimH*, and *rimA* [16] (Figure 2A), it was necessary to prevent polar effects on genes located downstream of the insertion point. The $ermE_P$ promoter, in the correct orientation to drive transcription of the messenger RNA, was therefore ligated upstream of the 582 bp SacII fragment internal to the coding region of *rimG* (coordinates 8267–8849 bp of the sequence deposited under accession number AY442225). The resulting construct was cloned in the PM1 phage vector in several steps described in Table 1; the resulting recombinant phage, PM1-768, carrying the desired construct was used to infect *S. diastaticus* var. 108, giving rise to lysogens *S. diastaticus* var. 108::PM1-768. Correct insertion into the chromosome was confirmed by Southern blotting. No tetraenes were detected in the fermentation broth when several lysogens were analyzed by HPLC, suggesting that low expression of the $ermE_P$ promoter was responsible for the nonproducer phenotype. Unfortunately, further attempts to disrupt *rimG* by using a stronger promoter ($ermE_P$*) were unsuccessful.

Two genes downstream of the insertion point could be influenced by the polar effect: *rimH* (coding for a ferredoxin, presumably participating in the same oxidative step as *rimG*) and *rimA* (coding for the PKS component carrying the loading domain of rimocidin [**3a**] and CE-108 [**4a**] (Figure 2A). Because the *rimH* product presumably acts in concert with that of *rimG*, it is reasonable that proper *rimA* expression would be the critical parameter for restoring formation of the polyene macrolides. In order to overcome this putative polar effect and assure proper expression of the *rimA* gene, the pSM743B plasmid (carrying an engineered *rimA*) was used. This plasmid was previously shown to be functional for both complementation of *rimA* disruption and induction of polyene amide formation [14]. pSM743B was therefore transferred by intraspecific

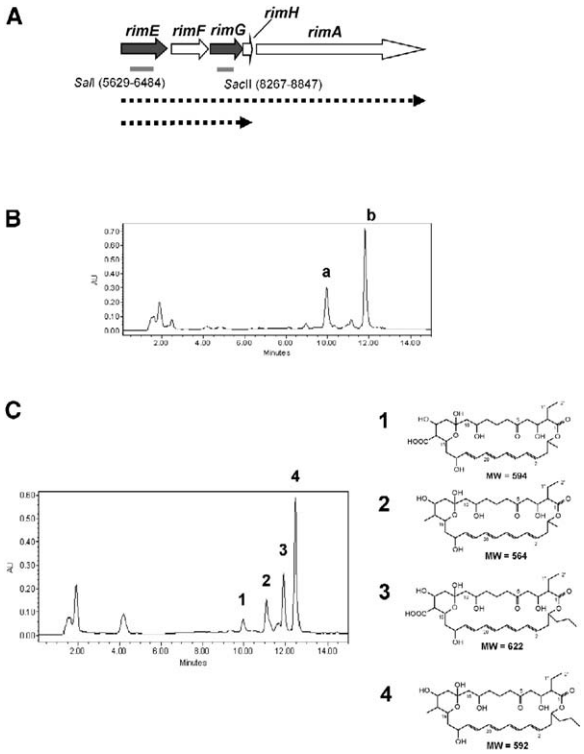

Figure 2. Disruption of *rimG* and *rimE* Genes

(A) Transcriptional organization of *rimE*, *rimF*, *rimG*, *rimH*, and *rimA* in this chromosomal region [16]. The deduced transcripts are represented by thick, dotted arrows. The DNA fragments used for insertional inactivation of the *rimG* and *rimE* genes are indicated by gray lines below them; the numbers within brackets refer to the DNA sequence deposited under accession number AY442225.

(B) HPLC analysis of the fermentation broth of *Streptomyces diastaticus* var. 108::PM1-768/743B. HPLC-MS analysis, carried out under analytical conditions (see Experimental Procedures), suggested for **a** and **b** the chemical structures corresponding to the methylated intermediates of the biosynthetic pathway of CE-108 and rimocidin, respectively (CE-108C [**4c**] and rimocidin C [**3c**]). Because no polyene amides were detected, it can be concluded that the side chain carboxylic group of the macrolactone ring is essential for polyene amide formation.

(C) HPLC analysis of the fermentation broth of the *rimE* disruptant. Left: chromatographic profile (under analytical conditions, see Experimental Procedures) of fermentation broth from *Streptomyces diastaticus* var. 108::PM1-702B/743B (see Table 1). Right: deduced chemical structures for the corresponding aglycones: CE-108 aglycone (**1**), CE-108C aglycone (**2**), rimocidin aglycone (**3**), and rimocidin C aglycone (**4**). It is noteworthy that the absence of polyene amides in the fermentation broth of this recombinant strain, in which the glycosyltransferase RimE is not present, strongly suggests that the native polyenes (CE-108 and rimocidin), but not their aglycones, are the substrates for the amidotransferase activity.

conjugation from the wild-type (*S. diastaticus* var. 108/743B) to the *rimG* disruptant, giving *S. diastaticus* var. 108::PM1-768/743B. Correct integration of PM1-768 into the genome of *S. diastaticus* var. 108 and the presence of the plasmid pSM743B were confirmed by Southern blotting and direct plasmid extraction, respectively.

When the fermentation broth of *S. diastaticus* var. 108::PM1-768/743B was analyzed by HPLC, two major compounds with the same spectrum and retention time as those of rimocidin (**3a**) and CE-108 (**4b**) were

Table 1. Bacterial Strains and Vectors Used in This Study

Strain, Plasmid, or Phage	Properties	Reference
E. coli JM101	General cloning host	[30]
Penicillium chrysogenum	For antifungal activity assays	ATCC10003
Candida albicans	For antifungal activity assays	ATCC10231
Candida krusei	For antifungal activity assays	ATCC14243
Aspergillus niger	For antifungal activity assays	ATCC1004
Cryptococcus neoformans	For antifungal activity assays	ATCC10226
S. lividans TK21	General cloning host	[28]
S. diastaticus var. 108	Wild-type (WT), CE-108, and rimocidin producer	[13]
S. diastaticus var. 108/KC859	WT derivative by integration of KC859 (WT, control)	[16]
S. diastaticus var. 108/PM1-768	WT derivative with *rimG* disrupted by integration of PM1-768	This work
S. diastaticus var. 108::PM1-768/743B	WT derivative with *rimG* disrupted by integration of PM1-768 and transformed with pSM743B; rimocidin C and CE-108C producer	This work
S. diastaticus var. 108/PM1-702B	WT derivative with *rimE* disrupted by integration of PM1-702B	This work
S. diastaticus var. 108::PM1-702B/743B	WT derivative with *rimE* disrupted by integration of PM1-702B and transformed with pSM743B	This work
S. diastaticus var. 108/PM1-500	WT derivative with *rimA* disrupted by integration of PM1-500	[16]
S. diastaticus var. 108::PM1-500/784	WT derivative with *rimA* disrupted by integration of PM1-500 and transformed with pSM784, tetraene nonproducer.	This work
pHJL401	Vector based on the SCP2* replicon and pUC19 replicon, *tsr*, 5.9 kb	[31]
pEL-1	EcoRI-HindIII fragment from pIJ4090 corresponding to $ermE_P$* [28] cloned in the EcoRI-HindIII sites of pHJL401	This work
PM1	ϕC31att$^-$ derivative, *hyg*, *tsr*	[32]
pSM743B	*rimA* under control of xylanase *xysA* promoter and *ermE* cloned into the EcoRV site of pIJ922	[14]
pCNB5006	Vector pIJ2925 carrying the $ermE_P$ promoter	[16]
pSM721	582-bp SacII internal fragment of *rimG* cloned into the HincII site of pIJ2925	This work
pSM768	HindIII-XbaI fragment from pSM721, carrying the 582 bp SacII internal fragment of *rimG* cloned into the BamHI-XbaI sites of pCNB5006	This work
PM1-768	1.0 kb BglII-PstI fragment from pSM768 cloned into the BamHI/PstI sites of PM1	This work
pEL-1/702	0.8 kb SalI internal fragment of *rimE* cloned into the BamHI site of pEL-1	This work
PM1-702B	1.1 kb EcoRI-XbaI fragment from pEL-1/702 cloned into the Ecl136II site of PM1	This work

Ap, ampicillin; *tsr* and *hyg*, thiostrepton and hygromycin resistance genes, respectively.

detected: peaks **a** and **b** (Figure 2B). HPLC-MS analysis showed that the deduced masses of peaks **a** and **b** were 709 and 737, 30 units lower than for CE-108 (**4a**) and rimocidin (**3a**). The mass differences are consistent with the expected structures of the compounds generated by *rimG* disruption: a methyl group at C-14 instead of the carboxyl group of CE-108 (**4a**) and rimocidin (**3a**). The two new, to our knowledge, tetraenes were named CE-108C (**4c**) and rimocidin C (**3c**) for the lower and higher retention time, respectively (Figure 1).

No polyene amides were detected in the fermentation broth of the *rimG* disruptant, in which a plasmid responsible for induction of polyene amides production in the wild-type strain is present; this finding strongly suggests that amide group formation takes place through a tailoring amidotransferase activity on the free carboxyl group rather than during assembly of the polyketide chain. Thus, the substrates for the tailoring amidotransferase reaction would be CE-108 (**4a**) and rimocidin (**3a**) and/or their respective aglycones.

rimE Gene Disruption

It remained unclear whether the substrates of the tailoring activity were CE-108 (**4a**) and rimocidin (**3a**) or their corresponding aglycones before glycosylation at C-17 with the mycosamine moiety.

In order to distinguish between these two possibilities, another disruptant of *rimE* (encoding the glycosyltransferase [16]) was made. To prevent possible polar effects on downstream genes, the fragment for disruption was engineered with $ermE_P$*, a stronger promoter than the $ermE_P$ previously used [16]. The 0.8 kbp SalI fragment internal to the coding region of *rimE* (coordinates 5629–6484 bp of the sequence AY442225) was first cloned into the pEL1 plasmid (Table 1) downstream of the $ermE_P$* promoter; and the *ermEp** promoter and the 0.8 kb SalI fragment (structurally similar to the previous construction with the $ermE_P$ promoter) were rescued and cloned into the PM1 vector. The resulting recombinant phage (PM1-702B) (see Table 1) was used to generate lysogens *S. diastaticus* var. 108/PM1-702B; the expected insertion was confirmed by Southern blotting. Fermentation broths from the lysogens were analyzed by HPLC (Figure 2C), and all of them showed the presence of four major peaks (1–4) with spectra corresponding to typical tetraenes. HPLC-MS analysis confirmed their masses. While peaks 1 and 3 showed the expected masses for the CE-108 (**4a**) and rimocidin (**3a**) aglycones, respectively, the masses for peaks 2 and 4 were consistent with those of the aglycones of CE-108 (**4a**) and rimocidin (**3a**), which carry a methyl side chain instead of the carboxyl group (see Figure 2C). These results were similar to those described in other glycosyltransferase disruptions [17]. No antifungal activity was detected for any of these aglycones, as previously described. These results strongly support the idea that the low production of these compounds in the former disruption was due

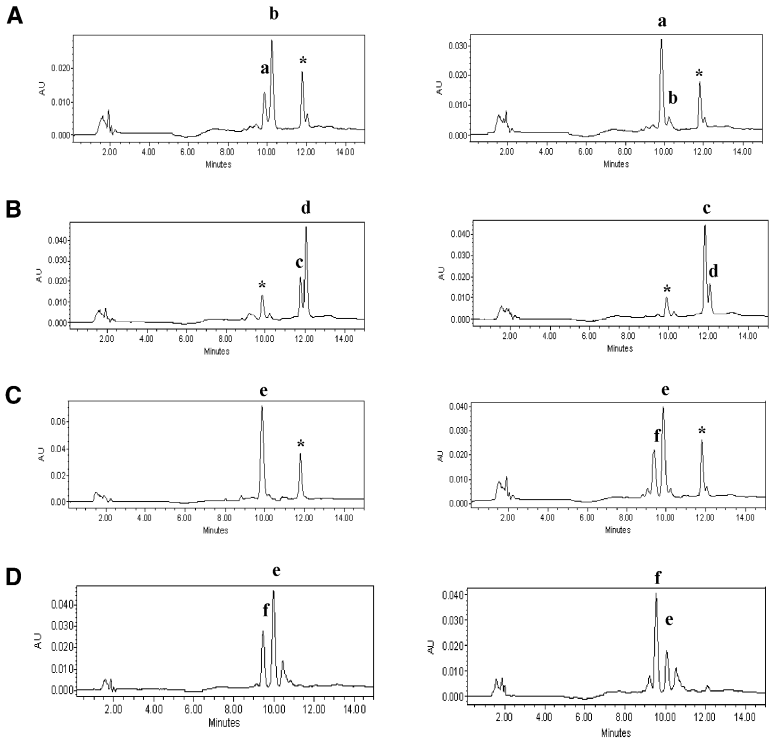

Figure 3. HPLC Analysis of In Vitro Amidotransferase Assays with Protein Extract from *Streptomyces diastaticus* var. 108/784 and *Streptomyces* sp. RGU5.3

(A–D) Assays with *Streptomyces diastaticus* var. 108/784 are shown in (A)–(C), and assays with *Streptomyces* sp. RGU5.3 are shown in (D). Chromatograms in the left and right columns show the products in the reaction mixture at the start time (t = 0) and after incubation (t = 60), respectively (times are expressed in min). The peaks are: (a) CE-108B (**4b**); (b), CE-108 (**4a**); (c), rimocidin B (**3b**); (d), rimocidin (**3a**); (e), pimaricin (**2a**), and (f), AB-400 (**2b**). (A) Enzymatic conversion of CE-108 (peak b) into its amide derivative CE-108B (peak a). Peak a and the peak marked with an asterisk at the start time are CE-108B and rimocidin B, respectively, and could not be completely removed in the protein extract. Note the increment of peak a (right panel) as the product of an amidotransferase activity. (B) Enzymatic conversion of rimocidin (peak d) into its amide derivative rimocidin B (peak c). Peak c and the peak marked with an asterisk at the start time are rimocidin B and CE-108B, respectively, and they are present in the protein extract. Similarly the product of the amidotransferase activity (peak c) (right panel) is significantly increased. (C) Enzymatic conversion of pimaricin (e) into its amide derivative, AB-400 (peak f). The peak marked with an asterisk is rimocidin B, which remains in the protein extract. Note the relaxed specificity of the amidotransferase from *S. diastaticus* var. 108/784 on the substrate recognition being able to convert a heterologous substrate (pimaricin) into its corresponding amide (AB-400). (D) Enzymatic conversion of pimaricin (e) into its amide derivative, AB-400 (f). The left and right chromatograms show the compounds in the reaction mixture at the start time (t = 0) and after incubation time (t = 60); peak f is AB-400, which is present in the protein extract, and e is pimaricin, which is added to the reaction mixture.

to low expression from the promoter used rather than to their chemical instability, as previously suggested [16].

Plasmid pSM743B (conferring the ability to produce the polyene amides when introduced into the wild-type strain [14]) was transferred by intraspecific conjugation into the *rimE* disruptant *S. diastaticus* var. 108/PM1-702B. The desired recombinant was selected by using the resistance markers and was confirmed by Southern blotting and plasmid extraction. The fermentation broth of the resultant strain (*S. diastaticus* var. 108::PM1-702B/743B) was subjected to HPLC-MS analysis, showing the same chromatographic profile as that of *S. diastaticus* var. 108/PM1-702B without pSM743B. The absence of polyene amides clearly suggests that the amidotransferase activity requires previous incorporation of mycosamine at C-17.

In Vitro CE-108 and Rimocidin Amidation Asssays

From the results described above, the polyene amides seem to be synthesized by a tailoring activity whose substrates would be the native tetraenes CE-108 (**4a**) and rimocidin (**3a**). In order to test for such activity in the fermentation broth of the polyene amide producer, *S. diastaticus* var. 108/784 (wild-type strain carrying a plasmid that confers the ability to produce the polyene amides [14]) was grown in SYM2 medium for 3 days. After testing by HPLC for production of the polyene amides, cell-free extracts were prepared as indicated in the Experimental Procedures. To prevent interference with the reaction products, most of the remaining polyenes still present in this preparation were removed by solid phase extraction with a Sep-Pak C18 cartridge (Waters). A set of preliminary reactions was assayed for polyene amide production in which several parameters were tested: substrates, cofactors, amide donors, and optimal pH (optimal amidotransferase activity was performed as described in Experimental Procedures). The reaction products were analyzed by HPLC. For a cleaner enzyme preparation, the pellets from several ammonium sulfate fractionations (25%, 45%, and 60% saturation) were assayed for activity and were shown to be associated with the 60% pellet. A clear conversion of both CE-108 (**4a**) and rimocidin (**3a**) was detected (Figures 3A and 3B). The identity of these peaks was confirmed by HPLC-MS analysis. No polyene amides were detected when ATP was absent from the enzyme reaction, suggesting that the amidotransferase activity is indeed an ATP-dependent reaction.

In Vitro Heterologous Amidation Asssay

To deduce the specificity of the polyene amidotranferase activity, pimaricin (**2a**) (Figure 1) and amphotericin B (**1**), along with CE-108 (**4a**) and rimocidin (**3a**) as control, were used as substrates in the amidotransferase reaction. The cell-free extracts and the reactions were performed as described in Experimental Procedures. As shown in Figure 3C, a protein extract from *S. diastaticus* var. 108/784 could also convert pimaricin (**2a**) into its corresponding amide, AB-400 (**2b**) (Figure 1) [18]. No conversion of amphotericin B (**1**) was detected,

suggesting that the amidotransferase from *S. diastaticus* var. 108 does not recognize **1** as a substrate under our experimental conditions. Cell-free extracts from *Streptomyces* RGU5.3 (recently characterized in our laboratory as producers of AB-400 [14]) were also tested for amidotransferase activity. In this strain, pimaricin (**2a**), not rimocidin (**3a**), CE-108 (**4a**), nor amphotericin B (**1**), could be converted into its corresponding amide under our experimental conditions, suggesting that this activity is more specific in substrate recognition than that of *S. diastaticus* var. 108 (see Figure 3D).

Characterization of Rimocidin C and CE-108C

Chemical Structure Elucidation

In order to verify the chemical structures of CE-108C (**4c**) and rimocidin C (**3c**), they were purified from the fermentation broth of *S. diastaticus* var. 108::PM1-768/743B by using a C8 reverse phase silica gel (see Experimental Procedures).

Compound **3c** was obtained as a yellow powder, which afforded pseudomolecular ions at *m/z* 738 ($[M+H]^+$) and 760 ($[M+Na]^+$) by (+)−ESI MS, according to the molecular formula $C_{39}H_{63}NO_{12}$ (by high-resolution MS found 738.442217, calcd. 738.442300 for $[M+H]^+$). Compared with the formula of **3a** ($C_{39}H_{61}NO_{14}$), this corresponds to the loss of two oxygen atoms and the addition of two protons in **3c**, which can formally be interpreted as an exchange of the carboxy group at C-14 against a methyl residue.

The ^{1}H NMR spectrum was very similar to that of rimocidin (**3a**) and displayed three signals in the sp^2 range, i.e., a doublet-of-doublet (dd) at δ 6.30, a multiplet at δ 6.05–6.18, and a second dd at δ 5.90 (Table 2). The protons of the sugar moiety appeared in the range of δ 3.25–4.62. The aliphatic region of the ^{1}H NMR spectrum also exhibited similarities with that of **3a**, especially with respect to five complex multiplet patterns in the range of δ1.30–2.50. Four methyl groups instead of three, as in **3a**, appeared as two triplets and two doublets at δ 0.90, 0.95 and 1.26, 1.00, respectively. The major difference between **3a** and **3c** was the presence of the methyl doublet at δ1.00, which showed an H,H crosssignal in the COSY spectrum with the 14-H at δ 1.22 (δ_C43.8).

The ^{13}C NMR spectrum indicated 39 carbon signals as in **3a** and as demanded by the molecular formula. This and the similarity of the proton spectra permitted the conclusion that **3a** and **3c** possess the same carbon skeleton, including the amino sugar, the only difference being the presence of only two carbonyl groups instead of three as in **3a**. The signals at δ 211.6 and 174.5 were attributed to a ketone and a lactone carbonyl, respectively. The HMBC ^3J coupling of the proton at δ 5.03 (C-27) to the carbonyl at 174.5 confirmed the lactone; thus, rimocidin C must be 14-decarboxy-14-methyl-rimocidin (**3c**).

The yellow powdery **4c** was readily soluble in methanol. Here too, the ^{1}H NMR spectrum exhibited similarities with those of **3c** and **4a** (Table 3; values from [13]), mainly in the aromatic and sugar region. The aliphatic region displayed the signals of four methyl groups as well—three doublets at δ 1.25, 1.23, and 0.99 and a triplet at 0.90—instead of three methyl signals as in **4a**. The (+)−ESI mass spectrum determined the molecular weight of **4c** as *m/z* 709, and high resolution delivered the molecular formula $C_{37}H_{59}NO_{12}$ (found 710.410905, calcd. 710.411000 for $[M+H]^+$). The ^{13}C NMR spectrum confirmed the presence of 37 carbon signals as in **4a** and as demanded by the molecular formula. Comparison with that of CE-108B (**4b**) revealed the presence of only two carbonyl signals at δ211.3 and 174.3, attributed again to a ketone and lactone carbonyl. The major difference here was the absence of the acid carbonyl, which appeared at δ 179.3 in **4a**, and the presence of an additional methyl signal at 13.7 that belongs to the methyl doublet at δ 0.99 in the ^{1}H NMR spectrum. A careful comparison of the data of **4a** and **4c** (Table 3) indicated clearly that, also in this tetraene, the C-14 carboxy group of **4a** was replaced by a methyl group, which identified CE-108C as the 14-decarboxy-methyl derivate **4a**.

Table 2. ^{1}H NMR and ^{13}C NMR Data of Rimocidin C in [D_4]Methanol

Position	^{1}H (Int., mult., *J* [Hz])	^{13}C
1	—	174.5
2	2.18 (1H, dt, 10.8, 3.6)	57.8
3	4.07 (1H, dd, 9.5, 2.4)	69.2
4	2.40; 2.46 (2H, m)	49.1
5	—	211.6
6	2.46; 2.30 (2H, m)	45.6
7	1.39 (2H, m)	19.5
8	1.30; 1.40 (2H, m)	38.3
9	3.80 (1H, m)	70.3
10	1.60 (2H, m)	48.8
11	—	98.7
12	1.96 (1H, dd, 4.6, 12.2), 1.26 (1H, m)	45.8
13	3.30[a] (1H, m)	71.8
14	1.22 (1H, m)	43.8
14-Me	1.00 (3H, d, 6.3)	13.7
15	3.91 (1H, tbr, 9.1)	71.3
16	2.20; 1.70 (2H, m)	38.6
17	4.42 (1H, tbr, 6.4)	78.7
18	5.90 (1H, dd, 15.2, 8.3)	137.4
19	6.30 (1H, dd, 14.5, 10.7)	134.4
20	6.11 (1H, m)	130.9*
21	6.11 (1H, m)	134.6*
22	6.11 (1H, m)	133.5*
23	6.11 (1H, m)	133.3*
24	6.11 (1H, m)	133.3*
25	5.60 (1H, m)	132.1
26	2.30; 2.50 (2H, m)	39.3
27	5.01 (1H, m)	74.8
28	1.62 (2H, d, 6.3)	38.1
29	1.40; 1.60 (2H, m)	20.5
30	0.95 (3H, d, 7.4)	14.2
1″	1.60; 1.90 (2H, m)	23.9
2″	0.90 (3H, t, 7.5)	12.3
Sugar Part		
1′	4.57 (1H, s)	99.5
2′	4.04 (1H, d, 2.3)	69.5
3′[b]	2.80 (1H, m)	57.4
4′[b]	3.58 (1H, m)	70.3
5′[b]	3.23 (1H, m)	74.6
6′	1.26 (3H, d, 5.5)	17.9

^{1}H NMR data of rimocidin C (**3c**) were collected at 600 MHz, and ^{13}C NMR data were collected at 150.8 MHz.
[a] Signals are partially overlapped by solvent.
[b] Tentatively assigned.

Biological Activities of Rimocidin C and CE-108C

Antifungal activity of the noncarboxylated tetraenes rimocidin C (**3c**) and CE-108C (**4c**) was tested against

Table 3. ^{1}H and ^{13}C NMR Data of CE-108 and CE-108C in [D_4]Methanol

Position	4a, ^{1}H, 500 MHz	4a, ^{13}C, 125.7 MHz	4c, ^{1}H, 600 MHz	4c, ^{13}C, 150.8 MHz
1	—	173.4	—	174.3
2	2.18 (1H, dt, 9.6, 3.8)	56.3	2.15 (1H, dt, 10.5, 3.7)	57.4
2″	1.59, 1.90 (2H, dq, 7.5, 3.8)	22.4	1.90, 1.59 (2H, 2 m)	21.0
2″-Me	0.92 (3H, t, 7.5)	10.9	0.90 (3H, t, 7.4)	12.0
3	4.11 (1H, dd, 9.6, 2.2)	68.5	4.07 (1H, dd, 10.6, 2.2)	69.4
4	2.37, 2.46 (2H, m)	48.8	2.44, 2.32 (2H, 2 m)	47.6
5	—	210.6	—	211.3
6	2.46, 2.32 (2H, m)	44.3	2.44, 2.32 (2H, 2 m)	45.2
7	1.39, 1.61 (2H, m)	19.6	1.38, 1.56 (2H, 2 m)	20.7
8	1.39, 1.30–1.26 (2H, m)	37.6	1.40–1.20 (2H, m)	38.3
9	4.12 (1H, ddt, 9.3, 8.2, 2.2)	68.4	3.56 (1H, ddd, 14.7, 10.8, 4.6)	70.1
10	1.61 (2H, m)	46.5	1.56 (2H, m)	45.8
11	—	97.8	—	98.7
12	2.02, 1.30–1.26 (2H, m)	44.1	1.96, 1.30–1.26 (2H, 2 m)	43.7
13	4.29 (1H, ddd, 11.1, 10.5, 4.6)	66.9	3.89 (1H, tbr, 9.1)	69.3
14	2.03 (1H, t, 9.3)	60.5	1.24 (1H, m)	38.6
14-COOH	—	179.3	—	—
14-Me	—	—	0.99 (3H, 6.3)	13.7
15	4.37 (1H, dd, 9.3, 8.2)	66.6	4.36 (1H, m)	69.4
16	2.30, 1.70 (2H, dd, 8.2)	38.7	2.32, 1.72 (2H, 2 m)	38.6
17	4.45 (1H, td, 3.5, 8.3)	78.2	3.83 (1H, m)	78.7
18	5.95 (1H, dd, 15.3, 8.3)	136.0	5.90 (1H, dd, 15.2, 8.3)	137.5
19	6.35 (1H, dd, 13.8, 10.7)	133.6	6.28 (1H, dd, 13.2, 10.8)	134.6
20	6.13 (1H, m)	129.3[a]	6.08 (1H, m)	130.7
21	6.13 (1H, m)	133.4[a]	6.08 (1H, m)	134.3
22	6.13 (1H, m)	132.3[a]	6.08 (1H, m)	133.5
23	6.13 (1H, m)	132.3[a]	6.08 (1H, m)	133.4
24	6.13 (1H, m)	132.6[a]	6.08 (1H, m)	133.3
25	5.63 (1H, ddd, 14.0, 9.5, 5.1)	131.1	5.61 (1H, m)	132.1
26	2.32, 2.40 (2H, m)	40.0	2.45, 2.30 (2H, 2 m)	40.9
27	5.07 (1H, ddq, 10.5, 6.3, 1.9)	70.8	5.04 (1H, ddq, 10.2, 6.3, 1.9)	71.8
28	1.26 (3H, d, 6.3)	20.0	1.23 (3H, d, 6.3)	20.4
Sugar				
1′	4.62 (1H, s)	98.2	4.51 (1H, sbr)	99.5
2′	4.03 (1H, d, 2.8)	68.0	4.05 (1H, d, 2.1)	70.3
3′	3.20 (1H, dd, 9.0, 2.8)	56.1	3.21 (1H, m)	57.4
4′	3.37[b] (1H, m)	69.5	3.26 (1H, m)	71.4
5′	3.35[b] (1H, m)	73.5	3.30[b] (1H, m)	74.6
6′	1.31 (3H, d, 5.7)	16.7	1.25 (3H, d, 5.9)	17.9

Signal intensity, multiplicity, and coupling constants are listed in brackets. The signals of **4c** were assigned tentatively according to the literature values of **4a**. See [13] for the ^{1}H and ^{13}C NMR data of CE-108.

[a] Tentatively assigned.

[b] The signal is partially overlapped by solvent.

several fungi—*Penicillium chrysogenum*, *Candida albicans*, *Aspergillus niger*, *Candida krusei*, and *Cryptococcus neoformans*—as previously described [14] and was compared with that of the native tetraenes. The antifungal activities of the two intermediate tetraenes, rimocidin C (**3c**) and CE-108C (**4c**), were not significantly different from those of their final products (data not shown).

To test whether or not other pharmacological properties of these tetraenes were different, hemolytic activity assays were also performed and compared with the parental compounds. Human erythrocytes were used for these assays; the results are shown in Table 4. It is noteworthy that, although the antifungal activities of **3a** and **3c** were similar, their toxicity (measured in terms of hemolytic activity) was 2.5- to 5-fold lower for rimocidin C (**3c**) than the parental rimocidin (**3a**). Up to 600 nanomols of CE-108C (**4c**) were used for the hemolytic assays; the detected hemolysis was less than 20% (data not shown), suggesting a much lower toxicity of the noncarboxylated CE-108 (**4c**) than for any of the other coproduced metabolites. This suggests an interesting improvement in biological properties.

Discussion

The polyene macrolides are a large group of compounds with interesting pharmacological properties, including potent antifungal activity, a broad antifungal spectrum, low probability of inducing resistance in the target strains, and a mechanism of action. These positive properties need to be set against negative ones such as high toxicity to mammals and very low water solubility. Because of the properties of some of these compounds, many approaches have been taken to generate new drugs: semisynthetic derivatives with more specific antifungal effects and higher water solubility [1, 6, 7, 10, 19], and genetic manipulation of biosynthetic genes [17, 20–22]. These two approaches face similar challenges: to increase the repertoire of these interesting compounds and improve the pharmacological properties of preexisting compounds as antifungal leads.

Table 4. Comparative Hemolytic Activity of Rimocidin, **3a**; Rimocidin C, **3c**; and CE-108, **4a**

	Rimocidin (**3a**)	Rimocidin C (**3c**)	CE-108 (**4a**)
20	15.55		
40	44.57		
60	73.82		
80	85.01		
100	100	8.27	
120		21.07	
140		53.96	7.83
160		78.92	17.03
200		84.7	22.64
240		100	24.29
280			37.95
320			57.8
360			67.72
400			86.12
440			100

The values tested for each tetraene are given in nanomols (left column), and the corresponding hemolytic activities are expressed as a percentage of total hemolysis. All of the values are the average of three independent assays.

A combination of both strategies is a promising tool for generating new pharmaceuticals.

In a previous report, we described two polyene compounds, rimocidin B (**3b**) and CE-108B (**4b**), produced by genetically modified *Streptomyces diastaticus* var. 108 [14]. Here, we show that these polyenes are derived from the parental compounds, rimocidin (**3a**) and CE-108 (**4a**), through modification by a tailoring ATP-dependent amidotransferase activity that converts the free carboxyl group into an amide group. Both polyenes, but not their aglycones, are substrates for such bioconversion. Under our experimental conditions, the enzyme system can also recognize the closely related polyene pimaricin (**2a**), but not amphotericin B (**1**). Although **2a** and **3a** are both tetraenes, their aglycones differ substantially: **3a** lacks the epoxy group of pimaricin (**2a**), and the C2 and C3 alkyl groups of **3a** are not present in **2a**. In contrast to the successful conversion by extracts of *S. diastaticus* var. 108/784, extracts of *Streptomyces* sp. RGU5.3, producer of AB-400 (**2b**, pimaricin amide) [14], did not catalyze the conversion.

The relaxed specificity in substrate recognition by the enzyme from *S. diastaticus* var. 108 is promising. We do not yet have enough experimental evidence to determine if the size of the macrolactone ring plays a critical role in substrate recognition. Therefore, the possibility of a successful enzymatic conversion of amphotericin B (**1**) into its amide derivative under different experimental procedures cannot be ruled out. More experimental work and/or eventually a properly engineered protein would be needed to gain insight into the critical parameters. Attempts are in progress to isolate the *S. diastaticus* var. 108 gene for amidotransferase activity. The possibility that this activity, properly engineered, could modify other polyenes is an exciting challenge for the near future; tools based on combinatorial biosynthesis will provide interesting opportunities for generating new polyene compounds with improved pharmacological properties by genetic engineering.

Based on sequence similarity with other monooxygenases such as PimG, NysN, and AmphN [23], we previously proposed that *rimG* would encode a cytochrome P450 monooxygenase involved in the conversion of the side chain methyl group of the macrolactone ring of **3a** and CE-108 (**4a**) into the free carboxylic acid [16]. Our experimental results confirm this prediction and confirm that the products accumulated by the *rimG* disruptants are rimocidin C (**3c**) and CE-108C (**4c**), the corresponding methylated polyene precursors, based on the finding that the C-14 methyl is not oxidized to the carboxyl group. The tetraene production profile observed in the *rimG* disruptant suggests that the carboxyl group is not required for attachment of mycosamine to the aglycone moiety and that the methylated CE-108 (**4c**) and rimocidin (**3c**) aglycones can also be substrates for transglycosylation. From the results of *rimE* and *rimG* disruption, we cannot establish the relative order in which those tailoring gene products (RimG and RimE) operate; a feedback inhibition of post-PKS tailoring steps as suggested by Chen et al. [17] cannot be excluded.

Despite the fact that the carboxyl group is highly conserved among polyenes, we provide evidence that this group is not essential for the biological activity of rimocidin and CE-108; moreover, its absence led to polyenes with lower toxicity compared with their oxidized counterparts. It is noteworthy that attempts to disrupt the corresponding monooxygenase gene in other polyene producers failed [24, 25]; there was no clear explanation. Nevertheless, the successful generation of the *amphN* mutant by means of an in frame deletion of the gene [26] has been recently reported and results in non-carboxylated amphotericin derivatives with similar biological properties as those described in this work. These findings create the exciting possibility that these intermediates may not be toxic for other producers as had been suggested [25]. Thus, the improved properties shown by these methyl-derived polyenes could also be shared by other polyenes. A targeted disruption of similar cytochrome P450 monooxygenase genes in other polyene biosynthetic clusters would provide an alternative way to generate new pharmaceutical leads.

To our knowledge, the tailoring activity described in this work is the first example of an enzyme involved in an in vivo chemical modification of the free carboxyl group of two typical polyenes into an amide group, a substitution that clearly increases selective toxicity toward ergosterol-containing membranes (more antifungal activity). Nevertheless, some other toxic effects unrelated to the membranes cannot be ruled out, and more work would be needed to test such possibility.

Significance

This work describes an amidotransferase activity involved in chemical modification of the free carboxyl group of two typical macrolide polyenes into an amide group, leading to improved pharmaceuticals. The relaxed specificity of this enzymatic activity, being able to modify pimaricin as well as CE-108 and rimocidin in vitro, creates the possibility of extending this modification in vivo to other polyene producers in an attempt to generate improved antifungal drugs. Disruption of *rimG*, encoding a P450 monooxygenase involved in free carboxyl group formation of rimocidin

and CE-108 tetraenes, allowed for the isolation of two noncarboxylated tetraenes with lower toxicity toward cholesterol-containing membranes. This finding creates the exciting possibility of obtaining other noncarboxylated polyenes with better pharmacological properties by disrupting a gene with a similar function in other polyene biosynthetic pathways.

Experimental Procedures

Bacterial Strains, Cloning Vectors, and Growth Conditions

The bacterial strains and plasmids are described in Table 1. *Streptomyces diastaticus* var. 108 and its derivatives were cultured in SYM2 medium [27]. *Streptomyces lividans* TK21 [28] was used for propagation of phages and as a cloning host. *E. coli* JM101 was grown on Luria-Bertani (LB) agar or in LB broth [29]. *Penicillium chrysogenum* ATCC10003 was used for testing antifungal activity and was grown in MPDA medium as previously described [16].

Genetic Procedures

E. coli JM101 was grown and transformed as described elsewhere [29]. *Streptomyces* strains were manipulated as described elsewhere [28]. Intraspecific conjugation was carried out as described previously [14]. DNA manipulations were performed as described by Maniatis et al [29].

Assay for Tetraenes Production under Analytical Conditions

The tetraene production assays were performed as previously described [16]. HPLC analyses for analytical purposes were carried out in all cases as described elsewhere [13].

HPLC-MS Assays

The mass spectra were determined on an 1100MSD HPLC connected to a quadrupole Agilent Technology Detector, by using electrospray as a source and a positive ionization mode. The chromatographic conditions were the same as those described above.

NMR Measurements

NMR spectra were measured on a Varian Inova 600 (599.740 MHz) spectrometer. ESI mass spectra were recorded on a Finnigan LCQ with quaternary pump Rheos 4000 (Flux Instrument). HR ESI mass spectra were measured on a Bruker FTICR 4.7 T mass spectrometer.

Purification of CE-108C and Rimocidin C

Streptomyces diastaticus var. 108::PM1-768/743B was grown on solid SYM2 medium supplemented with thiostrepton (50 μg/ml) and erythromycin (25 μg/ml) for selection of chromosomal insertion and plasmid markers, respectively. After 6 days, all of the solid medium was fragmented and processed as described previously [14]. CE-108C (**4c**) and rimocidin C (**3c**) were purified by HPLC by using a semipreparative column (Supelcosil PLC-8, 250 × 21.2 mm); the applied gradient was similar to that previously described for analytical fractionation [14] and was controlled with a Waters Automated Gradient Controller. The purified compounds were pooled and subjected to an additional desalting step with Sep-Pak C18 (Waters) cartridges and were finally freeze dried twice.

Hemolytic Activity Assay

The assays were carried out on human blood erythrocytes enriched as previously described [14].

Cell-free Extract Preparation and In Vitro Amidation Assays

Cell-free extracts were prepared from *Streptomyces diastaticus* var. 108/784 and *Streptomyces* sp. RGU5.3. The strains were grown in 50 ml SYM2 medium for 3 days. The mycelium was collected by centrifugation at 5,000 × g at 4ºC for 10 min, washed with 20% glycerol, and finally resuspended in 15 ml 20% glycerol. Aliquots of 500 μl were stored at −20ºC until use. When needed, the cells were pelleted by centrifugation and resuspended in 50 mM Tris-HCl (pH 7.5), 0.5 mM EDTA, 5% glycerol, 50 mM NaCl, 0.5 mM PMSF, and 1 mM β-mercaptoethanol (TEPM buffer). The cells were disrupted by sonication and centrifuged at 4,000 × g for 15 min at 4ºC, and the supernatant was again centrifuged. The polyenes contaminating the final supernatant were partially removed by passing the samples through Sep-Pak C18 (Waters) cartridges. The extracts were subjected to ammonium sulfate fractionation and raised sequentially to 45% and 60% ammonium sulfate saturation; the pellets were collected at 30,000 × g at 4ºC for 10 min and dissolved at 4-fold concentration in TEPM buffer. The pellet obtained at 60% ammonium sulfate saturation was used for the amidotransferase assays.

The amidotransferase assays were performed in 200 μl reaction containing 100 μl protein extract obtained as described above, 4×10^6 Units of Optical Density measured at 340 nm of the corresponding polyenes, 2.5 mM glutamine, 25 mM NaCl, 10 mM $MgCl_2$, 4 mM ATP, and 125 mM TES buffer (pH 7.2). The reactions were incubated at 30ºC for 60 min, were stopped by the addition of 1 volume of methanol, and were clarified by centrifugation at 4,000 × g, and the products were analyzed by HPLC. Rimocidin and CE-108, which were used as substrates for these reactions, were purified as previously described [14]; pimaricin and amphotericin B were purchased from Calbiochem (catalog nos. 527962 and 171375, respectively).

Acknowledgments

This work was supported by grants to F.M. from the Spanish Ministero de Ciencia y Tecnología BIO2002-01445. We thank Sir Prof. D.A. Hopwood for critically reading the manuscript.

Received: July 8, 2005
Revised: August 4, 2005
Accepted: August 8, 2005
Published: October 21, 2005

References

1. Baginski, M., Resat, H., and Borowski, E. (2002). Comparative molecular dynamics simulations of amphotericin B-cholesterol/ergosterol membrane channels. Biochim. Biophys. Acta *1567*, 63–78.
2. Cohen, B.E. (1998). Amphotericin B toxicity and lethality: a tale of two channels. Int. J. Pharm. *162*, 95–106.
3. Cohen, B.E., Ramos, H., Gamargo, M., and Urbina, J. (1986). The water and ionic permeability induced by polyene antibiotics across plasma membrane vesicles from *Leishmania sp*. Biochim. Biophys. Acta *860*, 57–65.
4. Saha, A.K., Mukherjee, T., and Bhaduri, A. (1986). Mechanism of action of amphotericin B on *Leishmania donovani* promastigotes. Mol. Biochem. Parasitol. *19*, 195–200.
5. Adjou, K.T., Demaimay, R., Deslys, J.P., Lasmezas, C.I., Beringue, V., Demart, S., Lamoury, F., Seman, M., and Dormont, D. (1999). MS-8209, a water-soluble amphotericin B derivative, affects both scrapie agent replication and PrPres accumulation in Syrian hamster scrapie. J. Gen. Virol. *80*, 1079–1085.
6. Chéron, M., Cybulska, B., Mazerski, J., Grzybowska, J., Czerwinski, A., and Borowski, E. (1988). Quantitative structure-activity relationships in amphotericin B derivatives. Biochem. Pharmacol. *37*, 827–836.
7. Cybulska, B., Bolard, J., Seksek, O., Czerwinski, A., and Borowski, E. (1995). Identification of the structural elements of amphotericin B and other polyene macrolide antibiotics of the hepteane group influencing the ionic selectivity of the permeability pathways formed in the red cell membrane. Biochim. Biophys. Acta *1240*, 167–178.
8. Cybulska, B., Gadomska, I., Mazerski, J., Borowski, J.G.E., Cheron, M., and Bolard, J. (2000). N-Methyl-N-D-fructosyl amphotericin B methyl ester (MF-AME), a novel antifungal agent of low toxicity: monomer/micelle control over selective toxicity. Acta Biochim. Pol. *47*, 121–131.
9. Graybill, J.R., Najvar, L.K., Fothergill, A., Hardin, T., Rinaldi, M., Lambros, C., and Regen, S.L. (1998). KY-62, a polyene analog of amphotericin B, for treatment of murine candidiasis. Antimicrob. Agents Chemother. *42*, 147–150.
10. Mazerski, J., Bolard, J., and Borowski, E. (1995). Effect of the modifications of ionizable groups of amphotericin B on its ability

to form complexes with sterols in hydroalcoholic media. Biochim. Biophys. Acta *1236*, 170–176.

11. Parmegiani, R.M., Loebenberg, D., Antonacci, B., Yarosh-Tomaine, T., Scupp, R., Wright, J.J., Chiu, P.J., and Miller, G.H. (1987). Comparative in vitro and in vivo evaluation of N-D-ornithyl amphotericin B methyl ester, amphotericin B methyl ester, and amphotericin B. Antimicrob. Agents Chemother. *31*, 1756–1760.
12. Szlinder-Richert, J., Mazerski, J., Cybulska, B., Grzybowska, J., and Borowski, E. (2001). MFAME, N-methyl-N-D-fructosyl amphotericin B methyl ester, a new amphotericin B derivative of low toxicity: relationship between self-association and effects on red blood cells. Biochim. Biophys. Acta *1528*, 15–24.
13. Pérez-Zúñiga, F.J., Seco, E.M., Cuesta, T., Degenhardt, F., Rohr, J., Vallín, C., Iznaga, Y., Pérez, M.E., González, L., and Malpartida, F. (2004). CE-108, a new macrolide tetraene antibiotic. J. Antibiot. (Tokyo) *57*, 197–204.
14. Seco, E.M., Cuesta, T., Fotso, S., Laatsch, H., and Malpartida, F. (2005). Two polyene amides produced by genetically modified *Streptomyces diastaticus* var. 108. Chem. Biol. *12*, 535–543.
15. Petkovic, H., Thamchaipenet, A., Zhou, L.H., Hranueli, D., Raspor, P., Waterman, P.G., and Hunter, I.S. (1999). Disruption of an aromatase/cyclase from the oxytetracycline gene cluster of *Streptomyces rimosus* results in production of novel polyketides with shorter chain lengths. J. Biol. Chem. *274*, 32829–32834.
16. Seco, E.M., Pérez-Zuñiga, F.J., Rolón, M.S., and Malpartida, F. (2004). Starter unit choice determines the production of two tetraene macrolides, rimocidin and CE-108, in *Streptomyces diastaticus* var. 108. Chem. Biol. *11*, 357–366.
17. Chen, S., Huang, X., Zhou, X., Bai, L., He, J., Jeong, K.J., Lee, S.Y., and Deng, Z. (2003). Organizational and mutational analysis of a complete FR-008/candicidin gene cluster encoding a structurally related polyene complex. Chem. Biol. *10*, 1065–1076.
18. Cañedo, L.M., Costa, L., Criado, L.M., Fernández Puentes, J.L., and Moreno, M.A. (2000). AB-400, a new tetraene macrolide isolated from *Streptomyces costae*. J. Antibiot. (Tokyo) *53*, 623–626.
19. Borowski, E. (2000). Novel approaches in the rational design of antifungal agents of low toxicity. Farmaco *55*, 206–208.
20. Brautaset, T., Bruheim, P., Sletta, H., Hagen, L., Ellingsen, T.E., Strom, A.R., Valla, S., and Zotchev, S.B. (2002). Hexaene derivatives of nystatin produced as a result of an induced rearrangement within the nysC polyketide synthase gene in *S. noursei* ATCC 11455. Chem. Biol. *9*, 367–373.
21. Byrne, B., Carmody, M., Gibson, E., Rawlings, B., and Caffrey, P. (2003). Biosynthesis of deoxyamphotericins and deoxyamphoteronolides by engineered strains of *Streptomyces nodosus*. Chem. Biol. *10*, 1215–1224.
22. Mendes, M.V., Recio, E., Fouces, R., Luiten, R., Martin, J.F., and Aparicio, J.F. (2001). Engineered biosynthesis of novel polyenes: a pimaricin derivative produced by targeted gene disruption in *Streptomyces natalensis*. Chem. Biol. *8*, 635–644.
23. Aparicio, J.F., Caffrey, P., Gil, J.A., and Zotchev, S.B. (2003). Polyene antibiotic biosynthesis gene clusters. Appl. Microbiol. Biotechnol. *61*, 179–188.
24. Caffrey, P., Lynch, S., Flood, E., Finnan, S., and Oliynyk, M. (2001). Amphotericin biosynthesis in *Streptomyces nodosus*: deductions from analysis of polyketide synthase and late genes. Chem. Biol. *8*, 713–723.
25. Fjaervik, E., and Zotchev, S.B. (2005). Biosynthesis of the polyene macrolide antibiotic nystatin in *Streptomyces noursei*. Appl. Microbiol. Biotechnol. *67*, 436–443.
26. Carmody, M., Murphy, B., Byrne, B., Power, P., Rai, D., Rawlings, B., and Caffrey, P. (2005). Biosynthesis of amphotericin derivatives lacking exocyclic carboxyl groups. J. Biol. Chem., in press. Published online August 3, 2005. 10.1074/jbc.M506689200.
27. Atlas, R.M. (1993). Microbiological Media (Boca Raton, FL: CRC Press).
28. Kieser, T., Bibb, M.J., Buttner, M.J., Chater, K.F., and Hopwood, D.A. (2000). Practical *Streptomyces* Genetics (Norwich, UK: John Innes Foundation).
29. Maniatis, T., Fritsch, E.F., and Sambrook, J. (1982). Molecular Cloning: A Laboratory Manual (Cold Spring Harbor, NY: Cold Spring Harbor Laboratory Press).
30. Yanisch-Perron, C., Vieira, J., and Messing, J. (1985). Improved M13 phage cloning vectors and host strains: nucleotide sequences of the M13mp18 and pUC19 vectors. Gene *33*, 103–119.
31. Larson, J.L., and Hershberger, C.L. (1986). The minimal replicon of a streptomycete plasmid produces an ultrahigh level of plasmid DNA. Plasmid *15*, 199–209.
32. Malpartida, F., and Hopwood, D.A. (1986). Physical and genetic characterisation of the gene cluster for the antibiotic actinorhodin in *Streptomyces coelicolor* A3(2). Mol. Gen. Genet. *205*, 66–73.